THE OFFICIAL MAGAZINE OF THE OCEANOGRAPHY SOCIETY

Oceanography

**CITATION**

Durack, P.J., P.J. Gleckler, S.G. Purkey, G.C. Johnson, J.M. Lyman, and T.P. Boyer. 2018. Ocean warming: From the surface to the deep in observations and models. *Oceanography* 31(2):41–51, https://doi.org/10.5670/oceanog.2018.227.

**DOI**

https://doi.org/10.5670/oceanog.2018.227

# Ocean Warming

## FROM THE SURFACE TO THE DEEP IN OBSERVATIONS AND MODELS

By Paul J. Durack, Peter J. Gleckler, Sarah G. Purkey, Gregory C. Johnson, John M. Lyman, and Tim P. Boyer

A CTD and water samples are recovered from over 4,000 m depth in Drake Passage by the British Antarctic Survey vessel RRS *James Clark Ross* in March 2013. These samples are part of the ongoing five-year joint US/UK Diapycnal and Isopycnal Mixing Experiment in the Southern Ocean (DIMES). *Photo credit: Andrew Meijers, BAS*

**ABSTRACT.** The ocean is the primary heat sink of the global climate system. Since 1971, it has been responsible for storing more than 90% of the excess heat added to the Earth system by anthropogenic greenhouse-gas emissions. Adding this heat to the ocean contributes substantially to sea level rise and affects vital marine ecosystems. Considering the global ocean's large role in ongoing climate variability and change, it is a good place to focus in order to understand what observed changes have occurred to date and, by using models, what future changes might arise under continued anthropogenic forcing of the climate system. While sparse measurement coverage leads to enhanced uncertainties with long-term historical estimates of change, modern measurements are beginning to provide the clearest picture yet of ongoing global ocean change. Observations show that the ocean is warming from the near-surface through to the abyss, a conclusion that is strengthened with each new analysis. In this assessment, we revisit observation- and model-based estimates of ocean warming from the industrial era to the present and show a consistent, full-depth pattern of change over the observed record that is likely to continue at an ever-increasing pace if effective actions to reduce greenhouse-gas emissions are not taken.

## INTRODUCTION

As the primary heat reservoir in the climate system, the ocean has absorbed more than 90% of Earth's anthropogenically added heat since 1971. Increasing anthropogenic greenhouse gases are the principal driver of the observed warming (Rhein et al., 2013), and this warming has contributed over 40% of global mean sea level rise since 1993 (WCRP Sea Level Budget Group, 2018). It has also led to substantial increases in the number and severity of marine heat waves, with serious consequences for ecosystems (e.g., Frölicher et al., 2018; Hobday et al., 2018, in this issue; Pershing et al., 2018, in this issue). Here, we focus primarily on ocean warming as a key indicator of climate change (e.g., von Schuckmann et al., 2016) and as a metric for climate model evaluation (Palmer, 2017).

While observed ocean warming has been replicated across many observational studies (e.g., Levitus et al., 2000; Ishii et al., 2003; Gouretski and Koltermann, 2007; Domingues et al., 2008; Palmer et al., 2009; Roemmich et al., 2015; Cheng et al. 2017; G.C. Johnson et al., 2018), the estimates do differ; accurate estimation of the human-forced changes that drive ocean warming is complicated by historical instrument biases (e.g., Gouretski and Koltermann, 2007; Lyman et al. 2010; Cheng et al., 2016a) as well as by sparse observing system coverage, especially prior to the advent of the Argo program in 2000 (Lyman and Johnson, 2014; Palmer, 2017). The upper ocean (0–700 m) is where the bulk of historical measurements exist and, consequently, where our knowledge of long-term change is most robust (Rhein et al., 2013). Over longer timescales, a consistent picture of forced ocean change is evident in ocean observations since initial assessments of global ocean warming were published (e.g., Levitus et al., 2000). Having ameliorated issues with data biases, many subsequent analyses present a clearer picture of change. The five estimates assessed document near-global upper-ocean warming from 1971 to 2010 at rates of 74–137 TW, with a representative mean warming rate of 107 TW. Although it likely occurred, there is less evidence of consistent warming before 1971 due to observational sparsity (Rhein et al., 2013). While there is considerably less data coverage for the intermediate (700–2,000 m) depths prior to modern Argo measurements (Lyman and Johnson, 2014), pentadal (five-year), estimates are available extending back to 1957 (Levitus et al., 2012). These also show marked warming over the observed record, but at a slower rate than in the upper ocean. Again, while all observed analyses show marked and statistically robust historical warming, their patterns and rates differ due to instrument biases, measurement coverage limitations, and the different methods and processing choices used to reconstruct global change estimates from sparse observations (e.g., Abraham et al., 2013; Boyer et al., 2016). These discrepancies largely disappear for the upper and intermediate ocean (0–2,000 m) in the modern Argo period up to the present (e.g., Roemmich et al., 2015; G.C. Johnson et al., 2018). However, it is important to note that the ice-covered polar regions and marginal seas are still not comprehensively sampled by Argo, although progress is ongoing with measurements in these regions.

In addition to observation-based estimates, model-observation syntheses or ocean "reanalyses" are now becoming available, providing model-constrained reconstructions of the observed record. While such syntheses are valuable, their differences highlight the uncertainties associated with the poorly observed pre-Argo period. Global ocean warming is reproduced by all ocean reanalyses, but over the poorly constrained historical period, the influence of model biases in the reanalysis systems lead to marked differences in the spatial patterns and consequently the temporal evolution of this signal differs markedly across the 19 products assessed by Palmer et al. (2017).

In this paper, we review the observed characteristics of ocean warming and report on published changes for the relatively well-investigated upper ocean. We also address recent results and model simulations that document significant changes in the deep ocean.

## THE OBSERVING NETWORK

Prior to Argo, and beneath the upper ocean (>700 m), historical observational coverage is markedly sparse. It is essentially based on hydrographic observations from ships (e.g., Durack et al., 2013) that began in the late 1800s, first using pressure-protected and then reversing pressure-protected thermometers (Abraham et al., 2013). Around the year 1900, reversing thermometers mounted on Nansen bottles came into use. From 1938, the mechanical bathythermograph

provided substantial amounts of upper-ocean temperature measurements, but with lesser accuracy. The development of the expendable bathythermograph (XBT) in the 1960s led to an increase in the amount of upper ocean temperature measurements, but again, these data were not of climate quality; poor data accuracy (the instrument required very careful calibration) limits their utility (Abraham et al., 2013). When electronics came to prominence in the 1960s, conductivity-temperature-depth sensors (CTDs) became popular, with the first profiles in the World Ocean Database available in 1961. CTDs quickly became the dominant source of high-quality data as their designs were improved, eventually eclipsing bottle profile counts in 1993 (Figure 1).

While large numbers of profiles have been recorded, they were mostly confined to the Northern Hemisphere, particularly the North Atlantic and along the western and eastern boundaries of the North Pacific (Figure 1B). The World Ocean Circulation Experiment (WOCE) aimed to address the spatial coverage biases with hydrographic transects conducted from 1990 to 1998 that provided a comprehensive baseline of densely sampled zonal and meridional sections gridding all three major ocean basins across both hemispheres. While WOCE resolved the spatial coverage issue, Southern Hemisphere seasonal coverage remained confined mostly to summer due to the sampling challenges in this harsh environment during winter.

Measurements from these sections provided a full ocean depth snapshot of temperature and salinity for the global ocean. Following the WOCE one-time hydrography program, a subset of 35 WOCE sections has been repeated roughly once a decade, first under the Climate and Ocean Variability, Predictability, and Change (CLIVAR/CO2) project and more recently under the Global Ocean Ship-Based Hydrographic Investigation Program (GO-SHIP; see Figure 5A, black lines). These repeated sections permit assessment of decadal temperature and salinity variability and change within the deep ocean basins.

During the WOCE era, the first iterations of autonomous profilers were being developed, and this led to the Argo Program beginning in 1999 (Gould et al., 2004; Riser et al., 2016). Argo now provides more than six times the total global profile coverage of all other observing platforms combined, reporting 175,998 temperature profiles in 2016 (Figure 1). A central goal of the Argo Program is ongoing collection and distribution of high-quality temperature and salinity observations in the upper 2 km for all of the ice-free open ocean (parts of the ocean with a bottom depth >2,000 m), in all seasons and without a spatial coverage bias. The successes of this revolutionary observing system solved longstanding issues of poor spatial and temporal data coverage in the discontinuous hydrographic observations from ships, especially the Northern Hemisphere coverage bias, by providing global measurements across the two hemispheres (Figure 1B). Although as previously noted, ice-dominated polar regions and marginal seas (such as those around Indonesia) are still not yet comprehensively covered by Argo, although progress in expanding Argo into these regions is ongoing.

Recent additional Argo initiatives include Biogeochemical Argo, which focuses on observing biologically relevant ocean properties such as oxygen, carbon dioxide, pH, and nitrate, with the first measurements recorded in 2003 (e.g., Kortzinger et al., 2005; K.S. Johnson et al., 2009), and Deep Argo (G.C. Johnson et al., 2015; Le Reste et al., 2016), which extends the physical observing array to 6,000 m, with the first Deep Argo floats deployed in 2012 and regional pilot arrays now in place (Jayne et al., 2017). Alongside these new platforms, there is ongoing work to better define platform metadata, quantify

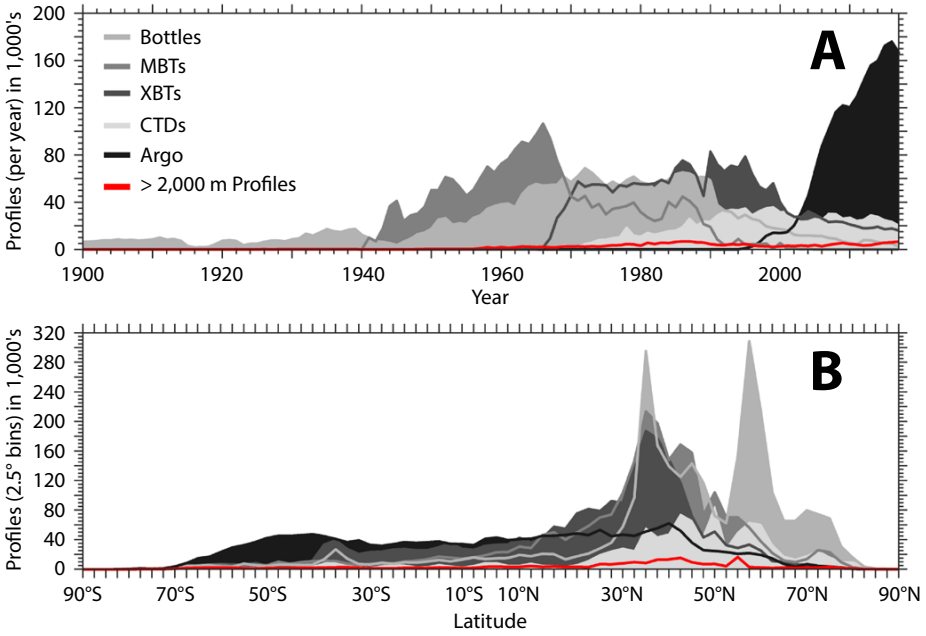


**FIGURE 1.** Ocean profile data from temperature observing platforms that comprise the World Ocean Database 2018 (Boyer et al., 2018). (A) Platform types for 1900 to 2018. (B) Presented in 2.5° zonal (latitude) bins for the period 1772 to 2018 (only 1900 onward shown). Shades of gray detail the five platforms used to measure temperature over the historical period. The red profiles indicate the number of total profiles from all platforms extending beneath 2,000 m depth. The global nature of the Argo program is evident in even distribution across both hemispheres, particularly when contrasted to bottles, which are the longest serving platform and which show a clear Northern Hemisphere bias over the complete coverage history (B). The Argo program captured almost 176,000 profiles in 2016, approaching three times more than bottles at their peak in 1972 (nearly 69,000 profiles) and almost five times more than CTDs at their peak in 1999 (see panel A).

uncertainties, and further improve estimates of ocean change from the existing historical measurement array (Domingues and Palmer, 2015).

## MODELS AS TOOLS

In parallel with improvements to the ocean observing system over recent decades, advancements have occurred in ocean model development, thanks to increasing computer power and the improved representation of ocean physics. Computational expansion has led to marked increases in resolution for some models so that they now approach eddy-permitting levels (~10 km) that begin to represent some aspects of the turbulent flows observed in nature. These higher resolution simulations can capture more of the cascading scales of ocean turbulence than their 1-degree (~100 km) predecessors, and this improved representation is believed to be important in order to simulate the key processes that drive ocean variability and change (see Penduff et al., 2018, in this issue). These continuous improvements in ocean model realism strengthen their utility for investigating the causes and effects of global and regional climate change. The improving observational data sets are also providing more rigorous benchmarks for evaluating the realism of ocean models. A recent comparison of a hierarchy of NOAA Geophysical Fluid Dynamics Laboratory (GFDL) ocean models (Griffies et al., 2015) illustrates the possibilities, with horizontal resolutions representing the Coupled Model Intercomparison Project Phase 5 (CMIP5; Taylor et al., 2012) contribution of 1-degree, through 0.25-degree, and down to an eddy-permitting 0.1-degree configuration. A comparison of maps of dynamic sea level height variability (captured in the measure of standard deviation) suggests a significant improvement in the 0.25-degree and 0.1-degree simulations, when contrasted to the much-muted result of the 1-degree simulation (Griffies et al., 2015).

For the CMIP5 archive, which mostly simulates Earth at coarser resolutions, Landerer et al. (2014) found that these models replicate the spatial gradients found in satellite estimates of sea surface height, a particularly relevant integrator of ocean processes that extend from the surface to the ocean floor, and thus were a marked improvement over their CMIP3 predecessors (Meehl et al., 2007). These models are also able to capture the large-scale regional aspects of global change, such as "polar amplification," with greater warming in polar waters than in the tropics reproduced in models similar to that shown in observations (e.g., Polyakov et al., 2002; Holland and Bitz, 2003; Cai, 2005; Gillett et al., 2008). As many of the CMIP6 (Eyring et al., 2016) contributing models are expected to further extend into higher resolution, improved realism in the next generation of the model suite is expected.

When comparing long-term changes in observations and models, it is useful to examine the more realistic CMIP5 *historical* simulations, in which climate models are forced with solar, greenhouse gas, natural and anthropogenic aerosol, and land use changes. These "forcing" data sets, which are derived from observed estimates, have been improving with time and, along with expansion of data sets, will enable increasing model complexity toward complete Earth system simulation (e.g., Durack et al., 2018). The historical simulations aim to capture forced contributions of the 1850 to 2005 observed climate. When compared with the variability and changes recorded across the numerous Earth observing systems, the model results provide insights into the forcing "causes" and resultant "effects" occurring concurrently across numerous characteristics of the climate system. Analyzing the large suite of models that contributed to CMIP5 enables us to examine the consistency of the simulated forced responses.

Even though the forcing data sets used in simulations are the best available at the time of their generation, some discrepancies exist with the real world due to uncertainties in the observed data coverage and the forcing data sets themselves (e.g., G.A. Schmidt et al., 2014). One example concerns volcanic aerosol forcing. Volcanoes emit sulfur dioxide, hydrochloric acid (HCl), and ash into the atmosphere. In most cases, the HCl condenses in water vapor and is rained out relatively quickly; however, the sulfur dioxide reacts to form sulfuric acid, which condenses and generates sulfate aerosols. In large volcanic eruptions, these aerosols find their way into the stratosphere where they reflect incoming solar radiation for more than a year, thereby exerting a cooling effect on Earth's climate. Stratospheric aerosols have been monitored since the early 1970s across numerous observing platforms, including satellites from 1979 to the present. Since the 2000s, the measurement of stratospheric aerosols has improved markedly, with new generation sensors and observing networks around the globe augmenting the monitoring capability.

It is now apparent that the volcanic forcing data used in the CMIP5 *historical* simulations did not accurately track real-world forcing. Discrepancies from around 1991 onward are apparent (e.g., Santer et al., 2014, 2017; G.A. Schmidt et al., 2014; A. Schmidt, 2018), with the stratospheric aerosol load dropping to background or zero values by 2000 and diverging from the observed conditions in which a series of late twentieth and early twenty-first century volcano eruptions occurred (Santer et al., 2014). This was one of several issues contributing to the discrepancy between the observed and modeled rate of global average surface warming for the 1998 to 2012 "hiatus" period (e.g., Flato et al., 2013; Medhaug et al., 2017; Liu and Xie, 2018, in this issue).

Despite these discrepancies, the 1998 to 2012 surface temperature warming rate is one of the most visible measures by which ongoing climate change is assessed. While surface warming is a highly visible metric of climate change,

other aspects of Earth's energy imbalance did not exhibit similar "hiatus" slowdowns during the same period. The ocean is the primary global heat sink due to the much larger capacity of water to absorb heat when compared to similar volume of air (the same energy increase that would raise global mean ocean temperatures by 0.001°C would raise the atmospheric temperature by 1.0°C), and therefore any changes to the ~0.7 W $m^{-2}$ rate of warming over the multidecadal observed period (Rhein et al., 2013; Palmer, 2017) would appear prominently in the global ocean heat content time series. In the ocean, there was no equivalent slowdown in the rate of heat absorbed, and this consistent warming is a feature that has persisted over the long term.

Model simulations provide one way to examine the full industrial-era (1870 to present) climate evolution. Gleckler et al. (2016) examined global ocean heat content changes for three distinct ocean layers, the upper (<700 m), intermediate (700–2,000 m), and deep (>2,000 m) ocean, with these layer separations motivated by the historical data depth coverage of the platforms that extend back to the 1950s and 1960s (see previous section on The Observing Network; Figure 1). This model-based analysis showed a strong simulated warming tendency, beginning with the upper ocean in 1920, the intermediate ocean around 1940, and the deep ocean around 1960, with a strong increase in the rate of warming since the 1960s, interspersed with warming slowdowns or reversals that were due to simulated forced volcanic eruptions (Figure 2A). As previously mentioned, volcanic eruptions that occurred since 2000 were omitted from the forcing data sets used to constrain the CMIP5 models. While it is impossible to accurately account for these unsimulated volcanic eruptions and their climate effects, subsequent work has estimated the effective forcing imposed by these twenty-first century volcanoes at −0.19 W $m^{-2}$ (Ridley et al., 2014). Using this estimate, we have corrected the 0 m to 2,000 m warming rates for the CMIP5 *historical* simulations (Figure 2B, black dashed line).

While measurement coverage is a problem over the long term (1960 onward), Argo provides global coverage from 2005 to the present day, and we can overlay the equivalent observed warming for five independent 2005 to 2017 ocean monthly reconstructions. When comparing the corrected upper to the intermediate model time series with modern observed data sets, they agree remarkably well, with strong agreement among the observed estimates showing a range of 3.6–5.0% $yr^{-1}$ that straddles the corrected model rate of 4.2% $yr^{-1}$ (Figure 2B).

## IMPLICATIONS OF HISTORICAL OBSERVATIONAL COVERAGE

While sparse coverage has led to considerable uncertainties in observed ocean properties over the historical period (e.g., Cheng and Zhu, 2014; Boyer et al., 2016; Wunsch, 2016), these uncertainties have been dramatically reduced in modern times. Following recent analyses of the historical uncertainties, the estimates of long-term ocean warming have been revised upward (e.g., Durack et al., 2014; Cheng et al., 2016b, 2017). The primary reasons identified for these revisions are insufficient spatial coverage of historical measurements (Lyman and Johnson,

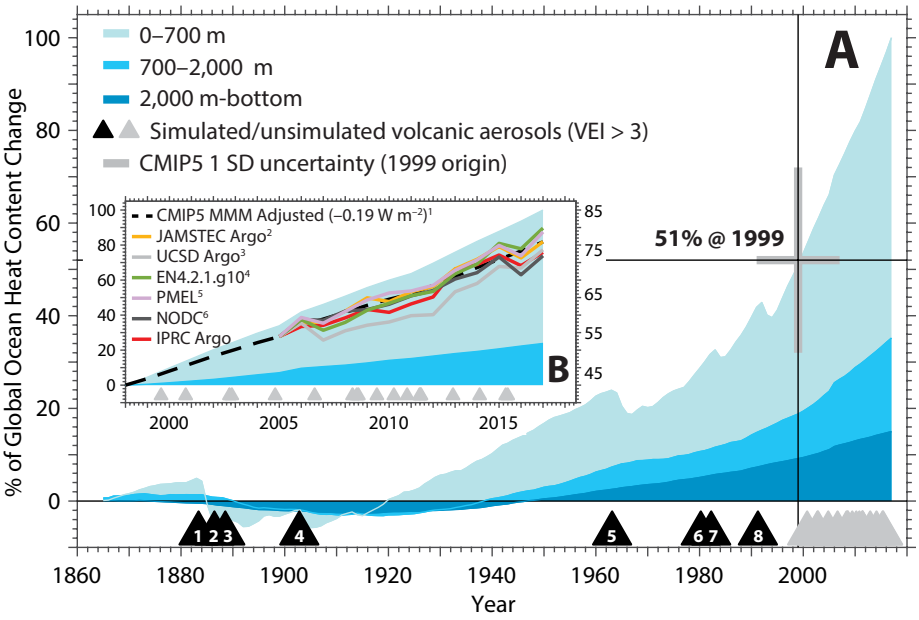


**FIGURE 2.** (A) Ocean models provide insights as to how the full-depth ocean responds to imposed simulated forcings and are useful tools to be used alongside observations. When contrasted over the modern Argo coverage, and corrected for discrepancies in forcing for the period from 2000 to near present, the model rate of change in ocean heat content approximates observed estimates. Ocean heat uptake (percentage of total 1865–2017 change) for the CMIP5 Multi-model Mean (MMM) layers are presented in the blue wedges for the deep (dark blue), intermediate (blue), and upper (cyan/light blue). The three shaded wedges are combined similarly to the IPCC Fifth Assessment Report (AR5) change in global energy inventory (Rhein et al., 2013, Box 3.1, Figure 1). The thick vertical gray bar represents a 1 standard deviation spread from the CMIP5 simulations for about the year (1997) when the MMM heat uptake reaches 50% of the net (1865–2017) industrial-era increase, and the thick horizontal gray bar indicates the CMIP5 1 standard deviation spread in the year when 50% of the total accumulated heat is reached. Black (forcing included) and gray (forcing not included) triangles represent major twentieth- and twenty-first-century volcanic eruptions with magnitudes represented by symbol size. *Figure adapted and updated from Gleckler et al., 2016* (B) Focusing on the well-observed modern period allows direct comparison of the rate of upper and intermediate ocean warming in models and observations. The plots show ocean warming (%) of the top 2,000 m for the period from 1998 to 2017, with the 2017 value representing 100%. The models used to generate panels A and B are documented in the online supplementary Table S2, and the observational data sets used are documented in Table S1.

[1] Ridley et al., 2014; [2] Hosoda et al., 2008; [3] Roemmich & Gilson, 2009; [4] Good et al., 2013; [5] Johnson et al., 2018; [6] Levitus et al., 2012

2014; Palmer, 2017) and platform biases. Most recently, much progress has been made through instrument bias corrections derived from careful intercomparisons of XBT data across different observing platforms (e.g., Cheng et al., 2016a). However, continuing work is required to further correct the remaining undocumented XBT profiles (approximately 50% of available profiles; e.g., Palmer et al., 2018) and to further investigate biases with the various mechanical bathythermograph platforms, which are presently not well understood. Continuing work on these issues will better quantify the current uncertainties associated with the historical record of ocean warming.

Considering the well-sampled modern Argo period, it is possible to assess how the broad-scale ocean heat content increase has continued, with an interesting example being the hemispheric partitioning of heat content change (e.g., Durack et al., 2014). This warming example has been highlighted in a modern assessment that shows 67%–98% of ocean warming over the 2006 to 2013 period occurring in the Southern Hemisphere extratropical ocean (south of 20°S) at a rate consistent with long-term estimates of 0.4–0.6 W $m^{-2}$ for the upper 2,000 m (Roemmich et al., 2015). We expanded this analysis to consider the 2005 to 2017 period, for which six independent ocean monthly reconstructions are available (Figure 3). The marked hemispheric asymmetry over this modern period is particularly striking, with a muted Northern Hemisphere ocean warming dwarfed by a very strong Southern Hemisphere ocean warming from 2007 to 2015 that is remarkably consistent across all six data products assessed. This agreement is captured in the range of trends for all six observational data products (not shown) that sit between 0.6–0.7 × $10^{22}$ J $yr^{-1}$ for the Southern Hemisphere, whereas all Northern Hemisphere data sets also show positive trends, albeit with less agreement over the period (0.13–0.36 × $10^{22}$ J $yr^{-1}$; see Figure 3), a result consistent with the work of Robson et al. (2016) who suggest this change is due to a reduction in the strength of the Atlantic Meridional Overturning Circulation. This hemispheric asymmetry peaks in 2015, with a consistent increase across all Northern Hemisphere data sets from 2015 to 2017, and a large coherent reduction followed by an increase for the Southern Hemisphere over the same 2015 to 2017 period (Figure 3).

Thanks to the near global coverage of Argo, it is also possible to map out the spatial patterns of heating over this 2005 to 2017 period (Figure 4). From these annual-mean trend maps, just like in the hemispheric integrals, it is clear that important features are shared across the data sets. The primarily small-scale differences in results can be attributed to multiple factors, including noisiness associated with sampling uncertainties and use of different analysis methods to reconstruct the time series, a situation very different from the disparities in both regional patterns and global mean values for the pre-Argo historical-period reconstructions (e.g., Boyer et al., 2016). The presented trends are all expressed as °C per decade (Figure 3) and such short timescales likely contain substantial decadal regional variability, so care must be taken when attempting to attribute such changes. For perspective, the mean warming over this relatively short period of data coverage for all products is ~0.05°C, with the largest magnitude changes in the northwest Atlantic reported by the IPRC analysis, approaching 0.7°C per decade (IPRC, 2015). One striking feature of their spatial distribution in this analysis is the strong and consistent pattern of warming across the Southern Ocean, particularly in the Indian and Atlantic subsectors (see Sallée, 2018, in this issue). Also, in the North Atlantic there is a prominent warming trend in the subtropics off the east coast of North America (noted above) and a cooling trend in the subpolar regions in all observational analyses. Both patterns are present in the CMIP5 maps across many historical and future simulations (Durack et al., 2014, their Figure S2B). The North Atlantic pattern has been linked to a

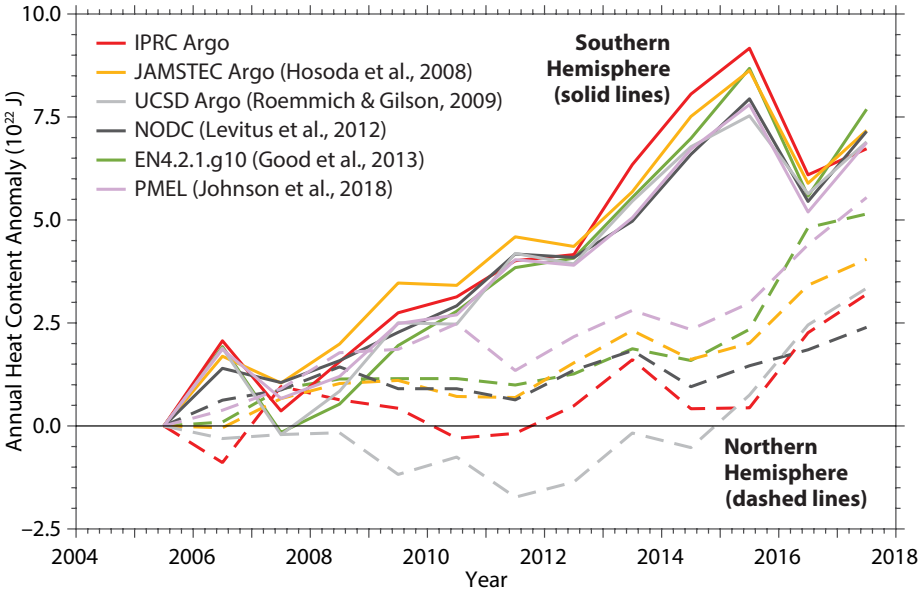


**FIGURE 3.** While limited observational coverage makes it difficult to accurately assess ocean heat content changes over the observed record, the Argo program provides near global 0 m to 2,000 m coverage since 2005. Comparison of hemispheric warming over the Argo period reveals strong asymmetry, with 67%–98% of warming over the 2006–2013 period occurring in the Southern Hemisphere (Roemmich et al., 2015) as shown very consistently across a suite of Argo (red, orange, and gray) and composite (green, black, and mauve) monthly gridded reconstructions. Units are J $10^{22}$ $yr^{-1}$. Colors used in this figure can be directly compared with time series in Figure 2B (inset). The data sets used are documented in Table S1.

reduction in strength of the observed Atlantic Meridional Overturning Circulation (e.g., Robson et al., 2016; Saba et al., 2016; Caesar et al., 2018), although the recent cooling appears attributable to extreme winter heat loss (Josey et al., 2018). Longer time series may be required to ascertain the primary drivers of these patterns and whether they are a manifestation of variability or a persistent change due to forcing.

## DEEP OCEAN CHANGE

Although considerable work has conclusively shown significant warming in the upper (<700 m) ocean where the bulk of historical ocean temperature measurements are found (e.g., Rhein et al., 2013, and the section above on The Observing Network), and extending down to 2,000 m during the recent Argo period, there is now a growing consensus supported by numerous studies that changes are also occurring in the deeper global ocean (>2,000 m). Based on observations below 2,000 m, it is estimated that the global ocean has accumulated heat at a rate of 33 ± 21 TW over 1991 to 2010 (Desbruyeres et al., 2016). Two-thirds of this warming is occurring between 2,000 m and 4,000 m, albeit with large uncertainty, almost entirely owing to warming in the Southern Ocean in this depth range (see Sallée, 2018, in this issue). Below 4,000 m, the observations show a large meridional gradient in the deep warming rate, with the southernmost basins warming 10 times faster than the deep basins to the north (Figure 5A). While the warming below 4,000 m only accounts for one-third of the total warming below 2,000 m, the regional variability is lower, leading to greater statistical certainty in the abyssal changes (4,000 m to 6,000 m; Purkey and Johnson, 2010; Desbruyeres et al., 2016; Figure 5A).

Despite their many limitations, global climate models are useful tools to complement available observations, particularly when examined in a large multimodel context such as CMIP5 where the consistency of the model responses to forcings can be examined more comprehensively. Using CMIP5 models, several studies have investigated deep ocean changes considering the strongly forced future projections (2006–2100) captured in the RCP26, RCP45, and RCP85 future experiments (e.g., Heuze et al., 2015; Rugenstein et al., 2016); the spatial patterns of these future changes agree well with the observed changes from the sparse observing network, albeit with much larger magnitudes. For this study,

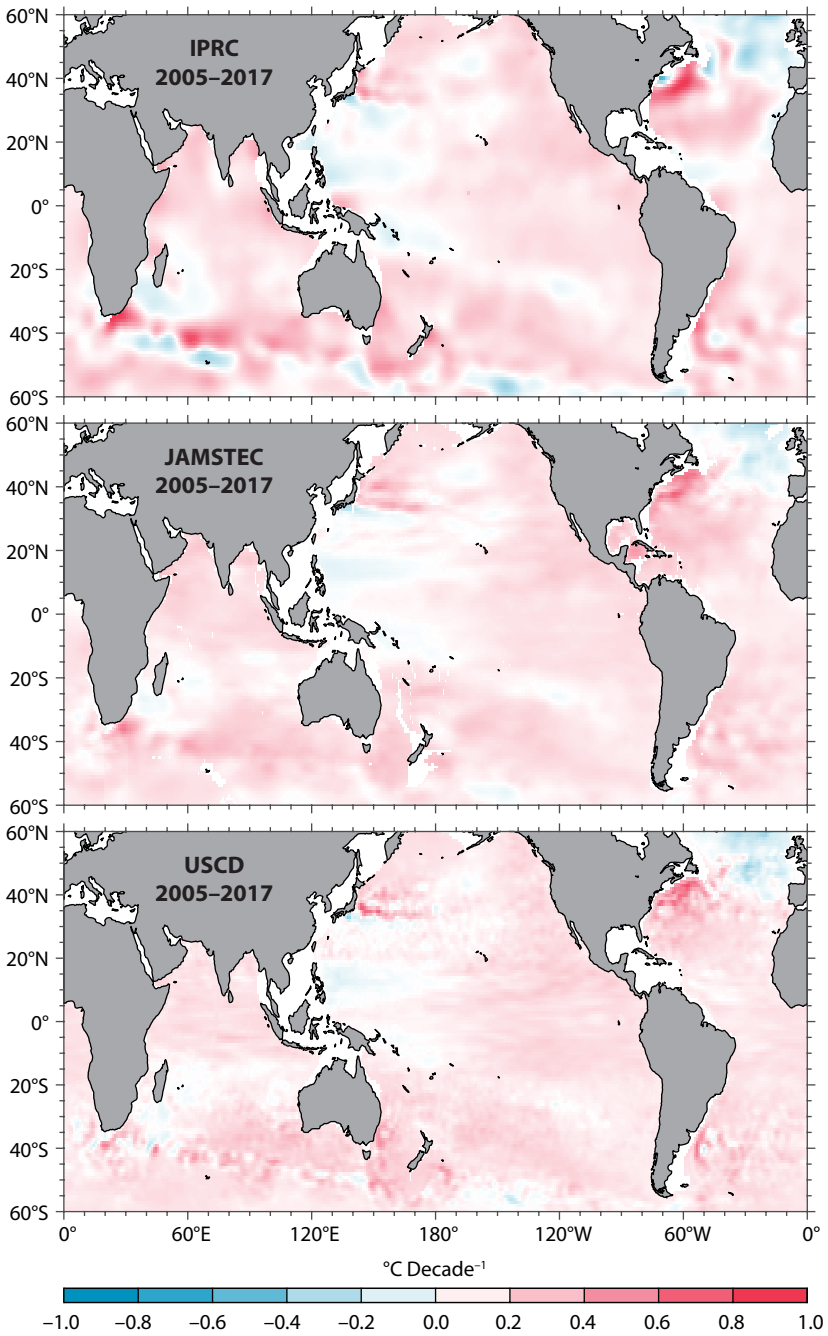


**FIGURE 4.** Three Argo reconstructions of 0 m to 2000 m depth-averaged ocean warming trends from 2005 to 2017; note that the maps extend from 60°N–60°S, and units are °C per decade. These reconstructions represent the geographical distribution of the composite hemispheric averages in Figure 3. While there are subtle differences between the three due to analysis choices, a strong and coherent warming signature is evident in the Southern Ocean along the flank of the Antarctic Circumpolar Current (40°–50°S), the eastern tropical Pacific Ocean, the northern Indian Ocean, and the northwest and southern Atlantic Ocean. The data sets used are documented in Table S1.

we presented new results focused on the 1950 to 2004 historical period over which the CMIP5 historical experiment was run, and observational estimates of change exist for both temperature (as noted above) and salinity (e.g., Durack and Wijffels, 2010). While the periods of comparison differ between observations (1990s to 2018) and the multidecadal timescale of the models, all changes are presented in units of °mC $yr^{-1}$, and so can be directly compared (Figure 5). Much like the observations, and the strongly forced future projections, a multi-model mean map of change expresses similar patterns of enhanced Southern Ocean warming, with the strongest patterns in the southern Indian and Atlantic sectors (Figure 5B; also see Sallée, 2018, in this issue). Consistency between models and observations is also evident in the reducing magnitudes of change in the northern basins, with a mixed (weakly positive and negative) result also presented for the North Atlantic (Figure 5). The observations show a slight cooling trend in the western Indian Ocean and a strong cooling feature in the southeast Atlantic Ocean not seen in the models. However, in observations, this cooling is not statistically different from zero, partially owing to insufficient data coverage in this region.

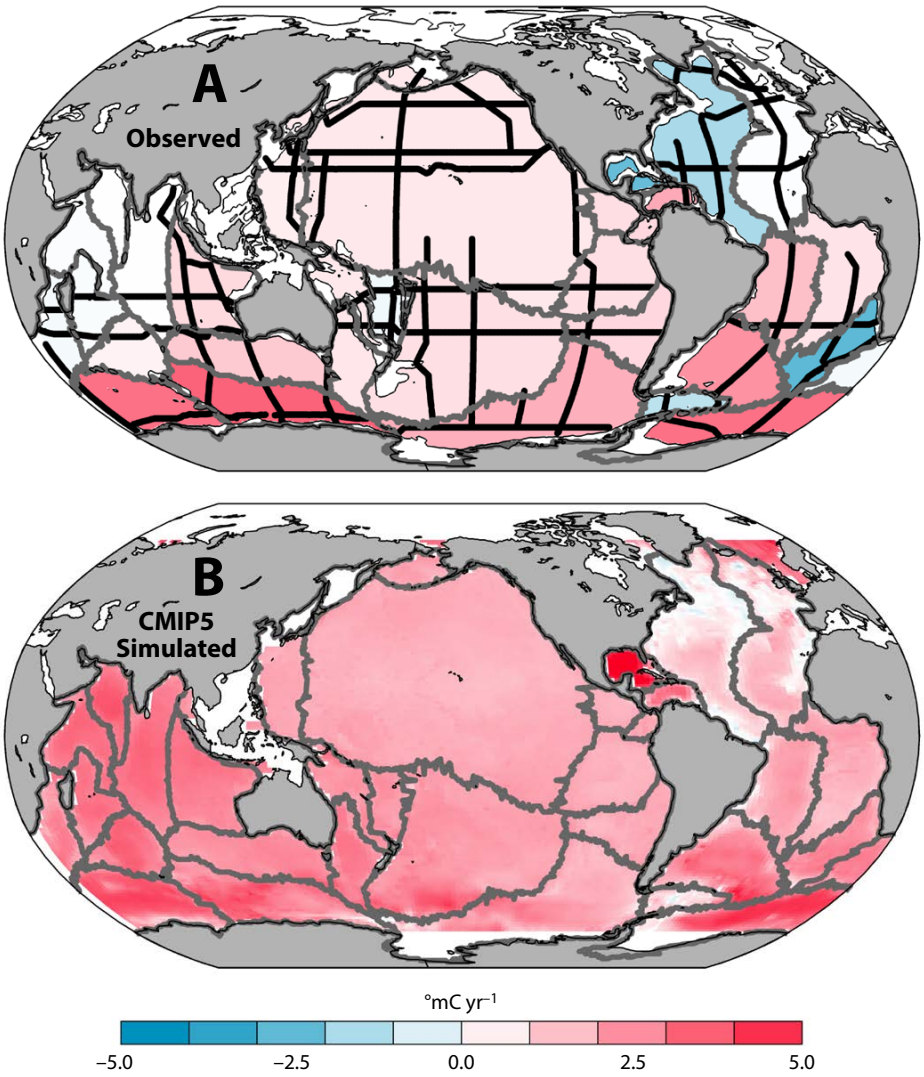


**FIGURE 5.** (A) While ocean observational coverage is even more sparse beneath 2,000 m, and is currently unsampled by Argo (see Figure 1), considerable deep warming has been observed between the 1990s and 2018 through repeated World Ocean Circulation Experiment/Global Ocean Ship-Based Hydrographic Investigations Program (WOCE/GO-SHIP) sections (black lines) within deep basins (gray lines). These observations (units °mC $year^{-1}$) show pronounced deep Southern Ocean warming that extends north into the Pacific, Atlantic, and Eastern Indian Oceans. There is cooling in the North Atlantic and possibly the Western Indian Oceans, although this cooling is not statistically different than zero owing to limited data (updated from Purkey and Johnson, 2010). (B) A multi-model mean with no such limitation for data coverage, of temperature change below 2,000 m between 1950 and 2004 (units are in °mC $yr^{-1}$) shows strong warming, evident for almost the entire ocean, except for the North Atlantic, with the strongest coherent warming signal across the Southern Ocean, similar to observations. While agreement is comforting, large differences in the patterns and magnitudes across single model ensemble members, and across individual models contributing to the multi-model mean map, are apparent, suggesting that internal climate variability and insufficient model physics both play strong roles over the comparatively weakly forced historical period. The models used to generate panel B are documented in Table S3.

While this agreement is suggestive of consistency between observations and models, we note that there are important differences in the spatial patterns among individual models. Deficiencies in the modeled physics at the relatively coarse resolution of CMIP5 models impact deep and especially bottom water formation simulation (Heuze et al., 2015; Newsom et al., 2016) and are almost certainly a culprit of observation-model differences, but there are other important limitations. Pattern differences in individual simulations from the same model suggest that internal climate variability in deep ocean property changes may also be an important factor. Limitations in the CMIP experimental design regarding the impact of volcanic forcings on pre-industrial control simulations may also play a role in model-observation differences (e.g., Gregory, 2010; Gregory et al., 2013). Finally, in the deep ocean, climate "drift" in some models may be of comparable magnitude to the signal of the relatively weakly forced historical simulations, and the method used to remove this imbalance can strongly influence the spatial patterns, thus adding uncertainty to the interpretation of the modeled results (e.g., Rahmstorf, 1995; Covey et al., 2006; Sen Gupta et al., 2012, 2013; Hobbs et al., 2016).

## SUMMARY

We have highlighted findings from many previous studies along with new results, all suggesting a marked warming signature in the global ocean extending from the surface to the abyss. These studies suggest that significant observed climate changes have already occurred, with both observations and model simulations suggesting a strong increase in the rate of change over recent decades. Model simulations of future projections suggest the rate of these changes will continue to increase markedly in coming decades, overwhelming the natural influences of volcanoes and unforced natural variability (Figure 2). Given that the global ocean is the primary heat reservoir in Earth's climate system, and that a prominent and increasing component of Earth's warming will likely be found in the deep ocean in coming decades (Palmer et al., 2011; Palmer and McNeall, 2014; von Schuckmann et al., 2016), it is critical that we maintain the current observational coverage and augment and expand it in coming years (e.g., Baker et al., 2007; Wunsch et al., 2013; NASEM, 2017; Stammer et al., 2018; Schmitt, 2018, in this issue). The new observing platforms Deep Argo and Biogeochemical Argo have much to offer; they will provide important further insights about ocean variability and change along with a concurrent assessment of biological aspects of ocean state such as changes to the oxygen inventory. However, we stress that these new platforms must complement and augment the existing observing capacity rather than compete with and replace the core physical Argo array that has been operating since 1999 (e.g., Durack et al., 2016). Maintenance of the ship-based GO-SHIP observing capacity is also a high priority, as this network provides the calibration bedrock for the new autonomous platforms, including both physical and biogeochemical water properties, along with the only available measurements of many oceanographic parameters, such as transient tracers, that can still only be analyzed from bottle samples.

Alongside the expanding observing capability, ocean reanalyses and the ocean component of climate models have considerably matured. The models and the improving forcing data sets that are used to reconstruct historical climate variability and change, used alongside observed reconstructions, provide a considerable toolkit to help tease apart the causes and effects of anthropogenic and natural forcing agents on ocean properties and drivers of long-term climate changes. Increases in model resolution will improve many aspects of ocean realism, such as representation of the meridional overturning circulation and eddy processes (e.g., Griffies et al., 2015; Newsom et al., 2016), and improvements in model physics will make these toolkits even more useful. However, the increasing volume of data being collected will likely also create new challenges for analysis. These tools provide extremely valuable insights into how our future world will look and what will be the consequences of a strong societal response, or lack of response, to the climate change challenge.

## SUPPLEMENTARY MATERIALS

Supplementary materials are available online at https://doi.org/10.5670/oceanog.2018.227.

## REFERENCES


Abraham, J.P., M. Baringer, N.L. Bindoff, T. Boyer, L.J. Cheng, J.A. Church, J.L. Conroy, C.M. Domingues, J.T. Fasullo, J. Gilson, and others. 2013. A review of global ocean temperature observations: Implications for ocean heat content estimates and climate change. *Reviews of Geophysics* 51(3):450–483, https://doi.org/10.1002/rog.20022.

Baker, D.J., R.W. Schmitt, and C. Wunsch. 2007. Endowments and new institutions for long-term observation. *Oceanography* 20(4):10–14, https://doi.org/10.5670/oceanog.2007.19.

Boyer, T.P., O.K. Baranova, C. Coleman, H.E. Garcia, A. Grodsky, R.A. Locarnini, A.V. Mishonov, T.D. O'Brien, C.R. Paver, J.R. Reagan, and others. 2018. *World Ocean Database 2018: Chapter 1. Introduction*. NOAA Atlas NESDIS NCEI, Silver Spring, Maryland, USA, https://data.nodc.noaa.gov/woa/WOD/DOC/wod_intro.pdf.

Boyer, T., C.M. Domingues, S.A. Good, G.C. Johnson, J.M. Lyman, M. Ishii, V. Gouretski, J.K. Willis, J. Antonov, S. Wijffels, and others. 2016. Sensitivity of global upper-ocean heat content estimates to mapping methods, XBT bias corrections, and baseline climatologies. *Journal of Climate* 29(13):4,817–4,842, https://doi.org/10.1175/JCLI-D-15-0801.1.

Caesar, L., S. Rahmstorf, A. Robinson, G. Feulner, and V. Saba. 2018. Observed fingerprint of a weakening Atlantic Ocean overturning circulation. *Nature* 556(7700):191–196, https://doi.org/10.1038/s41586-018-0006-5.

Cai, M. 2005. Dynamical amplification of polar warming. *Geophysical Research Letters* 32, L22710, https://doi.org/10.1029/2005GL024481.

Cheng, L., J. Abraham, G. Goni, T. Boyer, S. Wijffels, R. Cowley, V. Gouretski, F. Reseghetti, S. Kizu, S. Dong, and others. 2016a. XBT Science: Assessment of instrumental biases and errors. *Bulletin of the American Meteorological Society* 97(6):924–933, https://doi.org/10.1175/BAMS-D-15-00031.1.

Cheng, L., K.E. Trenberth, J. Fasullo, T. Boyer, J. Abraham, and J. Zhu. 2017. Improved estimates of ocean heat content from 1960 to 2015. *Science Advances* 3(3):e1601545, https://doi.org/10.1126/sciadv.1601545.

Cheng, L., K.E. Trenberth, M.D. Palmer, J. Zhu, and J.P. Abraham. 2016b. Observed and simulated full-depth ocean heat-content changes for 1970–2005. *Ocean Sciences* 12(4):925–935, https://doi.org/10.5194/os-12-925-2016.

Cheng, L., and J. Zhu. 2014. Artifacts in variations of ocean heat content induced by the observation system changes. *Geophysical Research Letters* 41(20):7,276–7,283, https://doi.org/10.1002/2014GL061881.

Covey, C., P.J. Gleckler, T.J. Phillips, and D.C. Bader. 2006. Secular trends and climate drift in coupled ocean-atmosphere general circulation models. *Journal of Geophysical Research* 111, D03107, https://doi.org/10.1029/2005JD006009.

Desbruyeres, D.G., S.G. Purkey, E.L. McDonagh, G.C. Johnson, and B.A. King. 2016. Deep and abyssal ocean warming from 35 years of repeat hydrography. *Geophysical Research Letters* 43(19):10,356–10,365, https://doi.org/10.1002/2016GL070413.

Domingues, C.M., J.A. Church, N.J. White, P.J. Gleckler, S.E. Wijffels, P.M. Barker, and J.R. Dunn. 2008. Improved estimates of upper-ocean warming and multi-decadal sea-level rise. *Nature* 453(7198):1,090–1,093, https://doi.org/10.1038/nature07080.

Domingues, C.M., and M.D. Palmer. 2015. The IQuOD initiative: Towards an international quality controlled ocean database. *CLIVAR Exchanges* 67(19, 2):38–40, http://www.clivar.org/documents/exchanges-67.

Durack, P.J., P.J. Gleckler, F.W. Landerer, and K.E. Taylor. 2014. Quantifying underestimates of long-term upper-ocean warming. *Nature Climate Change* 4(11):999–1,005, https://doi.org/10.1038/nclimate2389.

Durack, P.J., T. Lee, N.T. Vinogradova, and D. Stammer. 2016. Keeping the lights on for global ocean salinity observation. *Nature Climate Change* 6(3):228–231, https://doi.org/10.1038/nclimate2946.

Durack, P.J., K.E. Taylor, V. Eyring, S.K. Ames, T. Hoang, D. Nadeau, C. Doutriaux, M. Stockhause, and P.J. Gleckler. 2018. Toward standardized data sets for climate model experimentation. *EOS* 99, https://doi.org/10.1029/2018EO101751.

Durack, P.J., and S.E. Wijffels. 2010. Fifty-year trends in global ocean salinities and their relationship to broadscale warming. *Journal of Climate* 23:4,342–4,362, https://doi.org/10.1175/2010JCLI3377.1.

Durack, P.J., S.E. Wijffels, and T.P. Boyer. 2013. Long-term salinity changes and implications for the global water cycle. Pp. 727–757 in *Ocean Circulation and Climate: A 21st Century Perspective*. G. Siedler, S.M. Griffies, J. Gould, and J.A. Church,

eds, International Geophysics, vol. 103, Academic Press, Elsevier, Oxford, UK, https://doi.org/10.1016/B978-0-12-391851-2.00028-3.

Eyring, V., S. Bony, G.A. Meehl, C.A. Senior, B. Stevens, R.J. Stouffer, and K.E. Taylor. 2016. Overview of the Coupled Model Intercomparison Project Phase 6 (CMIP6) experimental design and organization. *Geoscientific Model Development* 9(5):1,937–1,958, https://doi.org/10.5194/gmd-9-1937-2016.

Flato, G., J. Marotzke, B. Abiodun, P. Braconnot, S.C. Chou, W. Collins, P. Cox, F. Driouech, S. Emori, V. Eyring, and others. 2013. Evaluation of climate models. Pp. 741–866 in *Climate Change 2013: The Physical Science Basis. Contribution of Working Group I to the Fifth Assessment Report of the Intergovernmental Panel on Climate Change*. T.F. Stocker, D. Qin, G.-K. Plattner, M. Tignor, S.K. Allen, J. Boschung, A. Nauels, Y. Xia, V. Bex, and P. M. Midgley, eds, Cambridge University Press, Cambridge, United Kingdom, and New York, NY, USA, https://doi.org/10.1017/CBO9781107415324.020.

Frölicher, T.L., E.M Fischer, and N. Gruber. 2018. Marine heatwaves under global warming. *Nature* 560(7718):350–364, https://doi.org/10.1038/s41586-018-0383-9.

Gillett, N.P., D.A. Stone, P.A. Stott, T. Nozawa, A.Y. Karpechko, G.C. Hegerl, M.F. Wehner, and P.D. Jones. 2008. Attribution of polar warming to human influence. *Nature Geoscience* 1(11):750–754, https://doi.org/10.1038/ngeo338.

Gleckler, P.J., P.J. Durack, R.J. Stouffer, G.C. Johnson, and C.E. Forest. 2016. Industrial-era global ocean heat uptake doubles in recent decades. *Nature Climate Change* 6(4):394–398, https://doi.org/10.1038/nclimate2915.

Good, S.A., M.J. Martin, and N.A. Rayner. 2013. EN4: Quality controlled ocean temperature and salinity profiles and monthly objective analyses with uncertainty estimates. *Journal of Geophysical Research*, 118(12):6,704–6,716. https://doi.org/10.1002/2013JC009067.

Gould, J., D. Roemmich, S. Wijffels, H. Freeland, M. Ignaszewsky, X. Jianping, S. Pouliquen, Y. Desaubies, U. Send, K. Radhakrishnan, and others. 2004. Argo profiling floats bring new era of in situ ocean observations. *EOS* 85(19):185–191, http://doi.org/10.1029/2004EO190002.

Gouretski, V., and K.P. Koltermann. 2007. How much is the ocean really warming? *Geophysical Research Letters* 34, L01610, https://doi.org/10.1029/2006GL027834.

Gregory, J.M. 2010. Long-term effect of volcanic forcing on ocean heat content. *Geophysical Research Letters* 37, L22701, https://doi.org/10.1029/2010GL045507.

Gregory, J.M., D. Bi, M.A. Collier, M.R. Dix, A.C. Hirst, A. Hu, M. Huber, R. Knutti, S.J. Marsland, M. Meinshausen, and others. 2013. Climate models without preindustrial volcanic forcing underestimate historical ocean thermal expansion. *Geophysical Research Letters* 40(8):1,600–1,604, https://doi.org/10.1002/grl.50339.

Griffies, S.M., M. Winton, W.G. Anderson, R. Benson, T.L. Delworth, C.O. Dufour, J.P. Dunne, P. Goddard, A.K. Morrison, A. Rosati, and others. 2015. Impacts on ocean heat from transient mesoscale eddies in a hierarchy of climate models. *Journal of Climate* 28(3):952–977, https://doi.org/10.1175/JCLI-D-14-00353.1.

Heuze, C., K.J. Heywood, D.P. Stevens, and J.K. Ridley. 2015. Changes in global ocean bottom properties and volume transports in CMIP5 models under climate change scenarios. *Journal of Climate* 28(8):2,917–2,944, https://doi.org/10.1175/JCLI-D-14-00381.1.

Hobbs, W., M.D. Palmer, and D. Monselesan. 2016. An energy conservation analysis of ocean drift in the CMIP5 global coupled models. *Journal of Climate* 29(5):1,639–1,653, https://doi.org/10.1175/JCLI-D-15-0477.1.

Hobday, A.J., E.C.J. Oliver, A. Sen Gupta, J.A. Benthuysen, M.T. Burrows, M.G. Donat, N.J. Holbrook, P.J. Moore, M.S. Thomsen, T. Wernberg, and D.A. Smale. 2018. Categorizing and naming marine heatwaves. *Oceanography* 31(2):162–173, https://doi.org/10.5670/oceanog.2018.205.

Holland, M.M., and C.M. Bitz. 2003. Polar amplification of climate change in coupled models. *Climate Dynamics* 21(3–4):221–232, https://doi.org/10.1007/s00382-003-0332-6.

Hosoda, S., T. Ohira, and T. Nakamura. 2008. A monthly mean dataset of global oceanic temperature and salinity derived from Argo float observations. *JAMSTEC Report of Research and Development* 8:47–59, https://doi.org/10.5918/jamstecr.8.47.

IPRC (International Pacific Research Center). 2015. Products based on Argo Data. Available online at http://apdrc.soest.hawaii.edu/projects/argo/.

Ishii, M., M. Kimoto, and M. Kachi. 2003. Historical ocean subsurface temperature analysis with error estimates. *Monthly Weather Review* 131(1):51–73, https://doi.org/10.1175/1520-0493(2003)131<0051:HOSTAW>2.0.CO;2.

Jayne, S.R., D. Roemmich, N. Zilberman, S.C. Riser, K.S. Johnson, G.C. Johnson, and S.R. Piotrowicz. 2017. The Argo program: Present and future. *Oceanography* 30(2):18–28, https://doi.org/10.5670/oceanog.2017.213.

Johnson, G.C., J.M. Lyman, T. Boyer, L. Cheng, C.M. Domingues, J. Gilson, M. Ishii, R. Killick, D. Monselesan, S.G. Purkey, and S.E. Wijffels. 2018. Global oceans: Ocean heat content. *State of the Climate in 2017*. *Bulletin of the American Meteorological Society* 99(8):S72–S77, https://doi.org/10.1175/2018BAMSStateoftheClimate.1.

Johnson, G.C., J.M. Lyman, and S.G. Purkey. 2015. Informing Deep Argo array design using Argo and full-depth hydrographic section data. *Journal of Atmospheric and Oceanic Technology* 32(11):2,187–2,198, https://doi.org/10.1175/JTECH-D-15-0139.1.

Johnson, K.S., W.M. Berelson, E.S. Boss, Z. Chase, H. Claustre, S.R. Emerson, N. Gruber, A. Kortzinger, M.J. Perry, and S.C. Riser. 2009. Observing biogeochemical cycles at global scales with profiling floats and gliders: Prospects for a global array. *Oceanography* 22(3):216–225, https://doi.org/10.5670/oceanog.2009.81.

Josey, S.A., J.J.-M. Hirschi, B. Sinha, A. Duchez, J.P. Grist, and R. Marsh. 2018. The recent Atlantic cold anomaly: Causes, consequences, and related phenomena. *Annual Review of Marine Science* 10:475–501, https://doi.org/10.1146/annurev-marine-121916-063102.

Kortzinger, A., J. Schimanski, and U. Send. 2005. High quality oxygen measurements from profiling floats: A promising new technique. *Journal of Atmospheric and Oceanic Technology* 22(3):302–308, https://doi.org/10.1175/JTECH1701.1.

Landerer, F.W., P.J. Gleckler, and T. Lee. 2014. Evaluation of CMIP5 dynamic sea surface height multi-model simulations against satellite observations. *Climate Dynamics* 43(5–6):1,271–1,283, https://doi.org/10.1007/s00382-013-1939-x.

Le Reste, S., V. Dutreuil, X. Andre, V. Thierry, C. Renaut, P.-Y. Le Traon, and G. Maze. 2016. "Deep-Arvor": A new profiling float to extend the Argo observations down to 4000-m depth. *Journal of Atmospheric and Oceanic Technology* 33(5):1,039–1,055, https://doi.org/10.1175/JTECH-D-15-0214.1.

Levitus, S., J.I. Antonov, T P. Boyer, O.K. Baranova, H.E. Garcia, R.A. Locarnini, A.V. Mishonov, J.R. Reagan, D. Seidov, E.S. Yarosh, and M.M. Zweng. 2012. World ocean heat content and thermosteric sea level change (0–2000 m), 1955–2010. *Geophysical Research Letters* 39, L10603, https://doi.org/10.1029/2012GL051106.

Levitus, S., J.I. Antonov, T.P. Boyer, and C. Stephens. 2000. Warming of the world ocean. *Science* 287(5461):2,225–2,229, https://doi.org/10.1126/science.287.5461.2225.

Liu, W., and S.-P. Xie. 2018. An ocean view of the global surface warming hiatus. *Oceanography* 31(2):72–79, https://doi.org/10.5670/oceanog.2018.217.

Lyman, J.M., S.A. Good, V.V. Gouretski, M. Ishii, G.C. Johnson, M.D. Palmer, D.A. Smith, and J.K. Willis. 2010. Robust warming of the global upper ocean. *Nature* 465(7296):334–337, https://doi.org/10.1038/nature09043.

Lyman, J.M., and G.C. Johnson. 2014. Estimating global ocean heat content changes in the upper 1800 m since 1950 and the influence of climatology choice. *Journal of Climate* 27(5):1,945–1,957, https://doi.org/10.1175/JCLI-D-12-00752.1.

Medhaug, I., M.B. Stolpe, E.M. Fischer, and R. Knutti. 2017. Reconciling controversies about the 'global warming hiatus.' *Nature* 545(7652):41–47, https://doi.org/10.1038/nature22315.

Meehl, G.A., C. Covey, T. Delworth, M. Latif, B. McAvaney, J.F.B. Mitchell, R.J. Stouffer, and K.E. Taylor. 2007. The WCRP CMIP3 multimodel dataset: A new era in climate change research. *Bulletin of the American Meteorological Society* 88(9):1,383–1,394, https://doi.org/10.1175/BAMS-88-9-1383.

National Academies of Sciences, Engineering, and Medicine. 2017. *Sustaining Ocean Observations to Understand Future Changes in Earth's Climate*. The National Academies Press, Washington, DC, https://doi.org/10.17226/24919.

Newsom, E.R., C.M. Bitz, F.O. Bryan, R. Abernathy, and P.R. Gent. 2016. Southern Ocean deep circulation and heat uptake in a high-resolution climate model. *Journal of Climate* 29(7):2,597–2,619, https://doi.org/10.1175/JCLI-D-15-0513.1.

Palmer, M.D. 2017. Reconciling estimates of ocean heating and Earth's radiation budget. *Current Climate Change Reports* 3(1):78–86, https://doi.org/10.1007/s40641-016-0053-7.

Palmer, M.D., T. Boyer, R. Cowley, S. Kizu, F. Reseghetti, T. Suzuki, and A. Thresher. 2018. An algorithm for classifying unknown expendable bathythermograph (XBT) instruments based on existing metadata. *Journal of Atmospheric and Oceanic Technology* 35(3):429–440, https://doi.org/10.1175/JTECH-D-17-0129.1.

Palmer, M.D., S.A. Good, K. Haines, N.A. Rayner, and P.A. Stott. 2009. A new perspective on warming of the global oceans. *Geophysical Research Letters* 36, L20709, https://doi.org/10.1029/2009GL039491.

Palmer, M.D., and D.J. McNeall. 2014. Internal variability of Earth's energy budget simulated by CMIP5 climate models. *Environmental Research Letters* 9(3):034016, https://doi.org/10.1088/1748-9326/9/3/034016.

Palmer, M.D., D.J. McNeall, and N.J. Dunstone. 2011. Importance of the deep ocean for estimating decadal changes in Earth's radiation balance. *Geophysical Research Letters* 38, L13707, https://doi.org/10.1029/2011GL047835.

Palmer, M.D., C.D. Roberts, M. Balmaseda, Y.-S. Chang, G. Chepurin, N. Ferry, Y. Fujii, S.A. Good, S. Guinehut, K. Haines, and others.

2017. Ocean heat content variability and change in an ensemble of ocean reanalyses. *Climate Dynamics* 49(3):909–930, https://doi.org/10.1007/s00382-015-2801-0.

Penduff, T., G. Sérazin, S. Leroux, S. Close, J.-M. Molines, B. Barnier, L. Bessières, L. Terray, and G. Maze. 2018. Chaotic variability of ocean heat content: Climate-relevant features and observational implications. *Oceanography* 31(2):63–71, https://doi.org/10.5670/oceanog.2018.210.

Pershing, A.J., K.E. Mills, A.M. Dayton, B.S. Franklin, and B.T. Kennedy. 2018. Evidence for adaptation from the 2016 marine heatwave in the Northwest Atlantic Ocean. *Oceanography* 31(2):152–161, https://doi.org/10.5670/oceanog.2018.213.

Polyakov, I.V., G.V. Alekseev, R.V. Bekryaev, U. Bhatt, R.L. Colony, M.A. Johnson, V.P. Karklin, A.P. Makshtas, D. Walsh, and A.V. Yulin. 2002. Observationally based assessment of polar amplification of global warming. *Geophysical Research Letters* 29(18):25-1–25-4, https://doi.org/10.1029/2001GL011111.

Purkey S.G., and G.C. Johnson. 2010. Warming of global abyssal and deep Southern Ocean waters between 1990s and 2000s: Contributions to global heat and sea level rise budgets. *Journal of Climate* 23(23):6,336–6,351, https://doi.org/10.1175/2010JCLI3682.1.

Rahmstorf, S. 1995. Climate drift in an ocean model coupled to a simple, perfectly matched atmosphere. *Climate Dynamics* 11(8):447–458, https://doi.org/10.1007/BF00207194.

Rhein, M., S.R. Rintoul, S. Aoki, E. Campos, D. Chambers, R.A. Feely, S. Gulev, G.C. Johnson, S.A. Josey, A. Kostianoy, and others. 2013. Observations: Ocean. Pp. 255–315 in *Climate Change 2013: The Physical Science Basis. Contribution of Working Group I to the Fifth Assessment Report of the Intergovernmental Panel on Climate Change*. T.F. Stocker, D. Qin, G.-K. Plattner, M. Tignor, S.K. Allen, J. Boschung, A. Nauels, Y. Xia, V. Bex, and P. M. Midgley, eds, Cambridge University Press, Cambridge, United Kingdom and New York, NY, USA, https://doi.org/10.1017/CBO9781107415324.010.

Ridley, D.A., S. Solomon, J.E. Barnes, V.D. Burlakov, T. Deshler, S.I. Dolgii, A.B. Herber, T. Nagai, R.R. Neely III, A.V. Nevzorov, and others. 2014. Total volcanic stratospheric aerosol optical depths and implications for global climate change. *Geophysical Research Letters* 41(22):7,763–7,769, https://doi.org/10.1002/2014GL061541.

Riser, S.C., H.J. Freeland, D. Roemmich, S. Wijffels, A. Troisi, M. Belbeoch, D. Gilbert, J. Xu, S. Pouliquen, A. Thresher, and others. 2016. Fifteen years of ocean observations with the global Argo array. *Nature Climate Change* 6(2):145–153, https://doi.org/10.1038/nclimate2872.

Robson, J., P. Ortega, and R. Sutton. 2016. A reversal of climatic trends in the North Atlantic since 2005. *Nature Geoscience* 9(7):513–517, https://doi.org/10.1038/ngeo2727.

Roemmich, D., J. Church, J. Gilson, D. Monselesan, P. Sutton, and S. Wijffels. 2015. Unabated planetary warming and its ocean structure since 2006. *Nature Climate Change* 5(3):240–245, https://doi.org/10.1038/nclimate2513.

Roemmich, D., and J. Gilson. 2009. The 2004–2008 mean and annual cycle of temperature, salinity, and steric height in the global ocean from the Argo Program. *Progress in Oceanography* 82(2):81–100, https://doi.org/10.1016/j.pocean.2009.03.004.

Rugenstein, M.A., A.J. Sedlacek, and R. Knutti. 2016. Nonlinearities in patterns of long-term ocean warming. *Geophysical Research Letters* 43(7):3,380–3,388, https://doi.org/10.1002/2016GL068041.

Saba, V.S., S.M. Griffies, W.G. Anderson, M. Winton, M.A. Alexander, T.L. Delworth, J.A. Hare, M.J. Harrison, A. Rosati, G.A. Vecchi, and R. Zhang. 2016. Enhanced warming of the Northwest Atlantic Ocean under climate change. *Journal of Geophysical Research* 121(1):118–132, https://doi.org/10.1002/2015JC011346.

Sallée, J.-B. 2018. Southern Ocean warming. *Oceanography* 31(2):52–62, https://doi.org/10.5670/oceanog.2018.215.

Santer, B.D., C. Bonfils, J.F. Painter, M.D. Zelinka, C. Mears, S. Solomon, G.A. Schmidt, J.C. Fyfe, J.N.S. Cole, L. Nazarenko, and others. 2014. Volcanic contribution to decadal changes in tropospheric temperature. *Nature Geoscience* 7(3):185–189, https://doi.org/10.1038/ngeo2098.

Santer, B.D., J.C. Fyfe, G. Pallotta. G.M. Flato, G.A. Meehl, M.H. England, E. Hawkins, M.E. Mann, J.F. Painter, C. Bonfils, and others. 2017. Causes of differences in model and satellite tropospheric warming rates. *Nature Geoscience* 10(7):478–485, https://doi.org/10.1038/ngeo2973.

Schmidt, A., M.J. Mills, S. Ghan, J.M. Gregory, R.P. Allan, T. Andrews, C.G. Bardeen, A. Conley, P.M. Forster, A. Gettelman, and others. 2018. Volcanic radiative forcing from 1979 to 2015. *Geophysical Research Letters*, https://doi.org/10.1029/2018JD028776.

Schmidt, G.A., D.T. Shindell, and K. Tsigaridis. 2014. Reconciling warming trends. *Nature Geoscience* 7(3):158–160, https://doi.org/10.1038/ngeo2105.

Schmitt, R.W. 2018. The ocean's role in climate. *Oceanography* 31(2):32–40, https://doi.org/10.5670/oceanog.2018.225.

Sen Gupta, A., N.C. Jourdain, J.N. Brown, and D. Monselesan. 2013. Climate drift in the CMIP5 models. *Journal of Climate* 26(21):8,597–8,615, https://doi.org/10.1175/JCLI-D-12-00521.1.

Sen Gupta, A., L.C. Muir, J.N. Brown, S.J. Phipps, P.J. Durack, D. Monselesan, and S.E. Wijffels. 2012. Climate drift in the CMIP3 models. *Journal of Climate* 25(13):4,621–4,640, https://doi.org/10.1175/JCLI-D-11-00312.1.

Stammer, D., A. Bracco, P. Braconnot, G.P. Brasseur, S.M. Griffies, and E. Hawkins. In press. Science directions in a post COP21 world of transient climate change: Enabling regional to local predictions in support of reliable climate information. *Earth's Future*, https://doi.org/10.1029/2018EF000979.

Taylor, K.E., R.J. Stouffer, and G.A. Meehl. 2012. An overview of CMIP5 and the experiment design. *Bulletin of the American Meteorological Society* 93(4):485–498, https://doi.org/10.1175/BAMS-D-11-00094.1.

von Schuckmann, K., M.D. Palmer, K.E. Trenberth, A. Cazenave, D. Chambers, N. Champollion, J. Hansen, S.A. Josey, N. Loeb, P.-P. Mathieu, and others. 2016. An imperative to monitor Earth's energy imbalance. *Nature Climate Change* 6(2):138–144, https://doi.org/10.1038/nclimate2876.

WCRP Global Sea Level Budget Group. 2018. Global sea-level budget 1993–present. *Earth System Science Data* 10:1,551–1,590, https://doi.org/10.5194/essd-10-1551-2018.

Wunsch, C. 2016. Global ocean integrals and means, with trend implications. *Annual Review of Marine Science* 8:1–33, https://doi.org/10.1146/annurev-marine-122414-034040.

Wunsch, C., R.W. Schmitt, and D.J. Baker. 2013. Climate change as an intergenerational problem. *Proceedings of the National Academy of Sciences of the United States of America* 110(12):4,435–4,436, https://doi.org/10.1073/pnas.1302536110.

## ACKNOWLEDGMENTS

Prepared by Lawrence Livermore National Laboratory (LLNL) under contract DE-AC52-07NA27344. The work of PJD and PJG is a contribution by LLNL to the science portfolio of the US Department of Energy, Office of Science, Climate and Environmental Sciences Division, Regional and Global Model Analysis Program. SGP was supported by National Science Foundation (NSF) grants OCE-1060804 and OCE-1437015. GCJ and JML are supported by NOAA Research and the NOAA Ocean Observations and Monitoring Division of the NOAA Climate Program Office (CPO-OOMD). TPB is supported by NOAA/NCEI and the NOAA CPO-OOMD and provided observational coverage data from the World Ocean Database 2018. LLNL Release Number: LLNL-JNRL-760809. PMEL Contribution number 4874.

## COMPETING INTERESTS

The authors declare that they have no competing financial interests.

## AUTHORS' CONTRIBUTIONS

PJD completed the analysis and shared responsibility for writing the manuscript. PJG, SGP, GCJ, JML and TPB shared responsibility for writing the manuscript.

## AUTHORS

**Paul J. Durack** (pauldurack@llnl.gov) is Research Scientist, and **Peter J. Gleckler** is Research Scientist, both at the Program for Climate Model Diagnosis and Intercomparison, Lawrence Livermore National Laboratory, Livermore, CA, USA. **Sarah G. Purkey** is Assistant Professor, Scripps Institution of Oceanography, University of California, San Diego, CA, USA. **Gregory C. Johnson** is Oceanographer, NOAA Pacific Marine Environmental Laboratory, Seattle, WA, USA. **John M. Lyman** is Assistant Researcher, NOAA Pacific Marine Environmental Laboratory, Seattle, WA, USA, and also at the Joint Institute for Marine and Atmospheric Research, University of Hawaii, Honolulu, HI, USA. **Tim P. Boyer** is Team Lead, Ocean Climate Laboratory Team, National Centers for Environmental Information (NCEI, formerly NODC), NOAA, Silver Spring, MD, USA.

## ARTICLE CITATION

Durack, P.J., P.J. Gleckler, S.G. Purkey, G.C. Johnson, J.M. Lyman, and T.P. Boyer. 2018. Ocean warming: From the surface to the deep in observations and models. *Oceanography* 31(2):41–51, https://doi.org/10.5670/oceanog.2018.227.